Device Modeling of an Optimized Monolithic All Lattice-Matched 3-Junction Solar Cell with Efficiency > 50%

Marina S. Leite[1,2,3] and Harry A. Atwater[1]

[1]Thomas Watson Laboratories in Applied Physics, California Institute of Technology, Pasadena, CA 91125, USA
[2]Center for Nanoscale Science and Technology, National Institute of Standards and Technology, Gaithersburg, MD 20899, USA
[3]Maryland Nanocenter, University of Maryland, College Park, MD 20742, USA

***Abstract* — Currently, there is a critical need for a photovoltaic design that will convert sunlight into electricity with practical efficiencies higher than 50%. Multijunction Solar Cells (MJSCs) are one of the most promising options to achieve ultra-high efficiencies. III-V compound semiconductors are generally used to fabricate MJSCs; however, limitations imposed by the lattice constants of available substrates strongly restrict which materials can be used for high-quality epitaxial growth. Herein we present an alternative design for an all lattice-matched monolithic 3-junction solar cell formed by (1.93 eV) InAlAs / (1.39 eV) InGaAsP / (0.94 eV) InGaAs, with 5.807 Å lattice constant. 1-dimensional device modeling for each individual subcell, as well as for the tandem device were performed under AM 1.5 direct illumination and concentrated sunlight. The role of concentration in each figure of merit was analyzed and Auger recombination was found to play an important role for high-injection levels. For a current match of 1.58 A/cm^2 we found that > 51% in efficiency can be achieved under 100-suns (with V_{oc} = 3.34 V). A detailed analysis of the effect of concentration on the device performance is presented.**

***Index Terms* — photovoltaic cells, semiconductor materials, modeling, solar energy, current-voltage characteristics.**

I. Introduction

Today, III-V compound semiconductors represent the best benefit/cost technology that can be achieved with concentrator photovoltaic (CPV) systems. The successfully implemented concept is based on multijunction solar cells (MJSCs). In such a device, each subcell is designed to have a specific bandgap in order to maximize the power conversion over the whole solar spectrum (Fig. 1a). There are basically two ways of splitting the spectrum in MJSCs into multiple segments. The first one is by using beam-splitting filters to efficiently distribute the light between all subcells, which allows for the use of independent single junction cells in a parallel, series, or another specific architecture. The second is to arrange the subcells in a mechanically-stacked configuration or a tandem system, in order of descending band gap energy so that the sunlight strikes the highest band gap subcell first. In this configuration, each subcell is united by a highly doped tunnel junction, which provides a low-resistance connection between the *p*-type base and the *n*-type emitter layers of the device (Fig. 1b).

Recently, distinct approaches for achieving ultra-high efficiencies using tandem solar cells have been suggested and successfully implemented. The first designs for triple- junction (3J) devices were based on GaAs and Ge substrates, due to the well-known optical and electronic properties of the lattice-matched heterostructures. Remarkable progress in the field led to efficiencies higher than 30% under 1-sun global illumination [1] and higher than 40% under concentrated direct sunlight [2], by using an inverted growth and a metamorphic bottom junction. More recently, bifacial epigrowth of InGaAs and InGaP/GaAs on GaAs was incorporated to achieve efficiencies higher than 42% under 406-suns illumination [3]. Additionally, dilute nitrides formed by GaInNAsSb have also been successfully implemented in 3-junction solar cells lattice-matched to GaAs, which have independently tunable band gaps and lattice constants [4]. To date, the world record 3-junction solar cell (43.5% under 418-suns illumination) utilizes this alloy as the middle 1 eV subcell, allowing for a better current match between the different subcells. All these approaches used either GaAs or Ge as a wafer for the epitaxial growth of the subcells. Nevertheless, distinct alloy combinations based on other substrates represent a promising pathway to achieve efficiencies higher than 50%. Quaternary alloys such as InAlAsSb and InGaAlAs lattice-matched to InP, combined with quantum wells, have been suggested as a possible design for 3J devices with theoretical efficiencies of 53% under AM1.5D 500-suns illumination [5].

II. An All Lattice-Matched Design

Our suggested pathway for a high efficiency lattice-matched monolithic 3J solar cell is formed by a combination of InAlAs/InGaAsP/InGaAs compound semiconductors (see Fig 1b). Ideally, this design can achieve efficiencies higher than 50% under 50-suns illumination (see Fig 1c), very promising for CPV. The optimized band gap energy combination (1.93 eV / 1.39 eV / 0.94 eV) corresponds to a lattice constant equal

to 5.807 Å [6]. The epitaxial growth of these alloys requires a crystalline template with same lattice constant, which is demonstrated elsewhere [7]. Our design allows for a very good current-match - the total current (J_{tot}) is equal to 15.3, 18.5, and 16.8 mA/cm^2, from top to bottom. As a proof of concept for the suggested multijunction design, we fabricated an equivalent 3J device lattice-matched to InP. These results were reported during the 37th IEEE PVSC [8]. The work presented here focuses on the device modeling of the lattice-matched monolithic optimized design, the performances of each individual subcell and of the 3J device under concentrated sunlight.

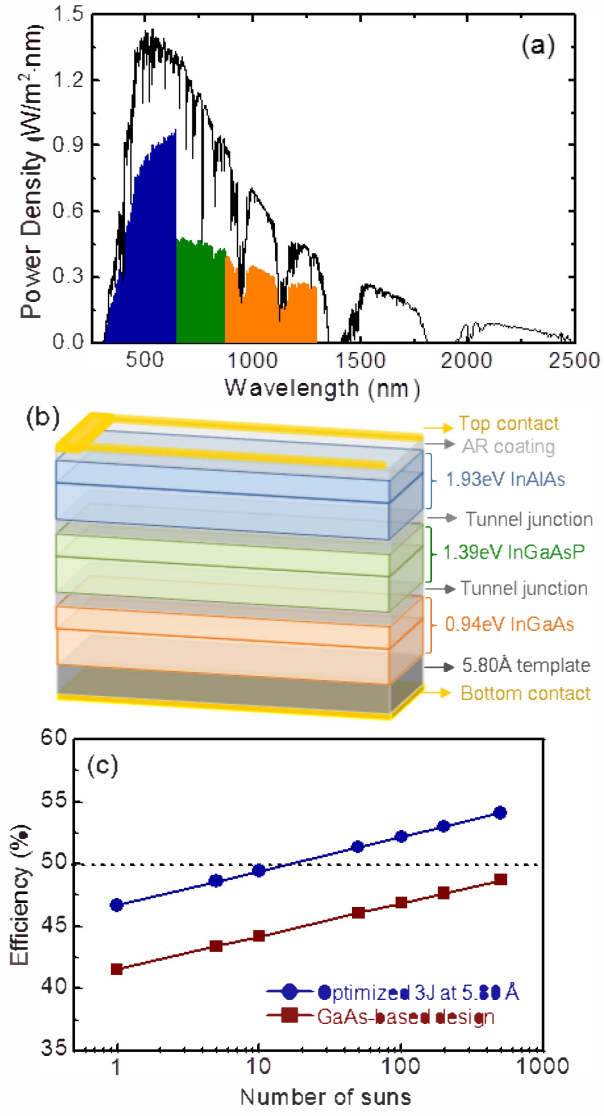

Fig. 1 (a) Power density of the sun as a function of wavelength at AM 1.5D illumination. The colored regions correspond to the wavelength absorbed by each subcell. (b) Schematic of a monolithic two-terminal series-connected (1.93 eV) InAlAs / (1.39 eV) InGaAsP / (0.94 eV) InGaAs 3-junction solar cell with an optimized bandgap energies combination, and lattice constant equal to 5.80 Å. The window layers are omitted and the layers are out of scale for clarity. (c) Efficiency vs. number of suns obtained by detailed balance calculation for the suggested 3-junction design and the GaAs-based conventional approach. All calculations were performed assuming constant temperature (300K). The suggested design can ideally achieve > 50% in efficiency under merely 50-suns illumination.

III. Device Modeling

Here, we use 1-dimensional device modeling in order to determine the performance of each individual subcell, as well as of the 3J device. The device modeling was performed using AFORS-HET [9], assuming Lambert-Beer absorption (no reflection losses), normal incidence of light, a *p*-type base and a *n*-type emitter for all subcells, abrupt *p*-*n* junctions, the occurrence of relaxation events, constant temperature (300K) and AM 1.5 direct 1-sun and concentrated illumination.

For every layer used in the device modeling we considered: material composition, thickness, dielectric constant, electron affinity, band gap, effective conduction and valence band densities, electron and hole motilities, the doping concentration of shallow acceptors and donors, the thermal velocity of electrons and holes, the alloy density, Auger recombination for electrons and holes, and direct band-to-band recombination. Additionally, we also took into account how many photons with a specific wavelength are absorbed and reflected by each layer based on its dielectric properties (*n*,*k*), which were used to calculate the corresponding spectral absorption coefficient. These values were calculated based on an ellipsometry database and by using Vegard's law for the layers at 5.807 Å.

Table 1 displays the composition, band gap energy, and thickness of each layer used in the simulations presented. The mechanical stack is formed by *p*-type bases and *n*-type emitters [Fig. 1(b)]. In all cases window and back surface field layers were used to reduce surface recombination and the scattering of carriers towards the tunnel junction, respectively. These layers were carefully chosen to be transparent to wavelengths absorbed by the subsequent lower band gap subcell.

The successful fabrication of the 1.93 eV InAlAs top subcell requires the growth of alloys with high Al content (0.63 in fraction for the *p*-*n* layers and 0.70 in fraction for the 2.1 eV window and back surface field layers) with a tensile strain of +0.47%. We have previously demonstrated the growth of dislocation-free epitaxial $In_{0.35}Al_{0.65}As/In_{0.52}Al_{0.48}As$ heterostructures with strain equal to +1.17% (2.5 times larger than what is required for the optimized top subcell) [8,10]. Therefore, a simple extension of the same MOVPE growth conditions should provide us high quality materials.

For both the middle and bottom subcells, lattice-matched window and back surface field layers with a band gap 0.5 eV

TABLE I

MATERIALS, BANDGAPS, AND THICKNESSES OF EACH SUBCELL FORMING THE LATTICE-MATCHED (1.93 eV) InAlAs / (1.39 eV) InGaAsP / (0.94 eV) InGaAs SETTINGS MONOLITHIC LATTICE-MATCHED 3-JUNCTION SUGGESTED DEVICE WITH OPITIMIZED BAND GAP COMBINATION. THE TUNNEL JUNCTIONS ARE OMITTED SINCE THE SIMULATIONS ASSUMED ZERO-RESISTANCE JUNCTIONS.

	Layer	Alloy	Eg (eV)	Thickness (μm)
Top subcell	Window	$In_{0.30}Al_{0.70}As$	2.10	0.02
	Emitter	$In_{0.37}Al_{0.63}As$	1.93	0.20
	Base	$In_{0.37}Al_{0.63}As$	1.93	2.50
	Back surface field	$In_{0.30}Al_{0.70}As$	2.10	0.02
Middle subcell	Window	$In_{0.37}Al_{0.63}As$	1.93	0.02
	Emitter	$In_{0.38}Ga_{0.62}As_{0.57}P_{0.43}$	1.39	0.20
	Base	$In_{0.38}Ga_{0.62}As_{0.57}P_{0.43}$	1.39	2.00
	Back surface field	$In_{0.37}Al_{0.63}As$	1.93	0.02
Bottom subcell	Window	$In_{0.85}Ga_{0.15}P$	1.43	0.02
	Emitter	$In_{0.38}Ga_{0.62}As$	0.94	0.20
	Base	$In_{0.38}Ga_{0.62}As$	0.94	2.50
	Back surface field	$In_{0.85}Ga_{0.15}P$	1.43	0.02

higher than that of the *p-n* absorber layer are available, as shown in Table 1.

Current-matching was enforced between the individually modeled subcells. For the presented design the top subcell was found to be the limiting one for 1-sun illumination, as a result of the lower total current. The assumption of zero-loss tunnel junctions is reasonable due to the fact that an InP-based fabricated tandem multijunction solar cell presented the same performance as the equivalent independently-connected subcells, as reported elsewhere [8].

The potentiality of the suggested design lies on the fact that the modeled device showed efficiency $\eta > 40\%$ under 1-sun illumination – see Fig 2. This value is significant lower than the detailed balance result [~ 47%, see Fig 1(c)] due to the consideration of Auger and other recombination phenomena. This result also indicates that the device modeling presented here is fairly realistic.

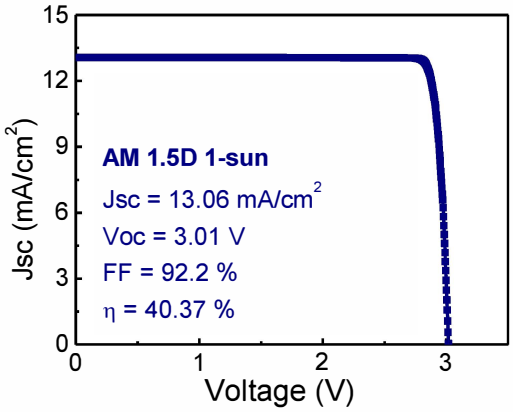

Fig. 2 Modeled light J-V curve for the all lattice-matched (1.93eV) InAlAs / (1.39eV) InGaAsP / (0.94eV) InGaAs monolithic 3-junction device obtained from 1-dimensional device modeling for AM 1.5 direct illumination, assuming Lambert-Beer absorption, normal incidence of light, recombination processes, zero-loss tunnel junctions, and 300K.

IV. PERFORMANCE UNDER CONCENTRATION

Since only direct light can be effectively focused on CPV systems we analyze the effect of illumination concentration (α) on the performance of the 3J design. The figures of merit for the 3J device were individually calculated and analyzed (see Table 2 and Fig 3). At low injection, by increasing the incident flux of light by α, the short circuit current (J_{sc}) increases linearly at a first approximation, as $J_{sc}(\alpha) \approx \alpha \cdot J_{sc}$. For each subcell the open circuit voltage (V_{oc}) increases as a logarithmic function of α, as a result of free carrier generation enhancement as:

$$V_{oc}(a) \approx \frac{kT}{e} ln\left(\frac{aJ_{sc}}{J_o} + 1\right)$$

$$V_{oc}(a) \approx V_{oc}(1) + \frac{kT}{e} ln(a) \quad (1)$$

where k is Boltzmann's constant, T is the temperature of the cell, J_o is a constant, $V_{oc}(1)$ is the open circuit voltage under 1-sun illumination, and e is the electron charge. Thus, at 10-suns illumination, the V_{oc} of the 3J device improves by 180 mV, corresponding to an increase of 60mV for each subcell. The

TABLE II

FIGURES OF MERIT FOR THE LATTICE-MATCHED (1.93eV) InAlAs / (1.39eV) InGaAsP / (0.94eV) InGaAs IGURES MONOLITHIC 3-JUNCTION DEVICE OBTAINED FROM 1-DIMENSIONAL DEVICE MODELING FOR AM 1.5 DIRECT ILLUMINATION, ASSUMING LAMBERT-BEER ABSORPTION, NORMAL INCIDENCE OF LIGHT, ZERO-LOSS TUNNEL JUNCTIONS, AND TEMPERATURE = 300K.

# of suns	J_{sc} *(A/cm²)*	V_{oc} *(V)*	*FF (%)*	η *(%)*
1	0.013	3.01	92.2	40.37
10	0.130	3.19	92.3	42.76
20	0.261	3.24	92.3	43.42
50	0.653	3.30	92.1	44.14
100	1.306	3.35	91.6	44.46
200	2.613	3.39	90.3	44.34
500	6.533	3.43	85.4	42.58

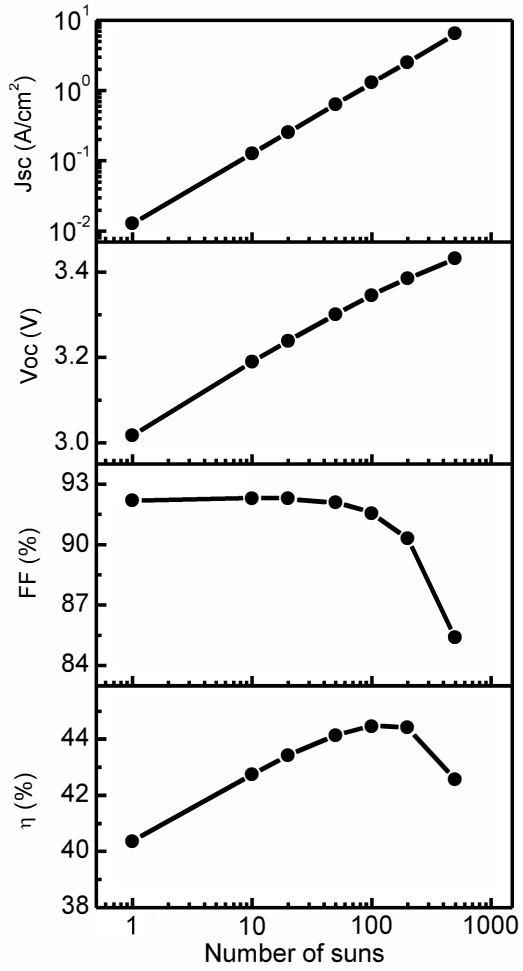

Fig. 3 Figures of merit for the optimized lattice-matched 3-junction device as a function of illumination (number of suns). Data obtained from 1-dimensional device modeling, using direct illumination.

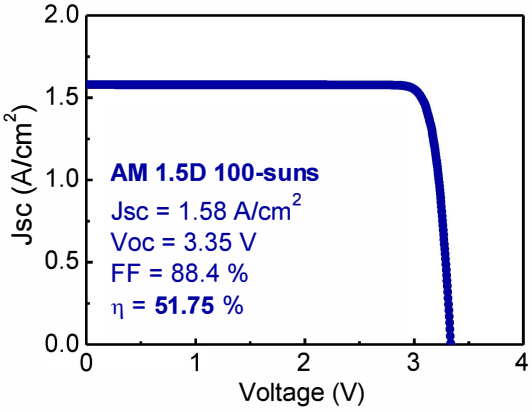

Fig. 4 Light J-V curve for an optimized (1.93eV) InAlAs / (1.39eV) InGaAsP / (0.94eV) InGaAs obtained from 1-dimensional full device modeling using AM 1.5 direct 100-suns illumination, assuming zero-resistance tunnel junctions between the subcells. Note that >51% in efficiency is achieved for concentration illumination after re-optimization of the top InAlAs subcell.

boost in the V_{oc} is greater for low-bandgap subcells. As shown by the simulations, at 100-suns illumination, the V_{oc} improves by 12% (around 10% for the top and middle subcells, and 20% for the bottom one, in agreement with eq. 1).

However, at high injection levels (α > 100 in this case) Auger recombination is dominant, resulting in an increase in the dark current and a lower enhancement in V_{oc}. This non-linear electronic relaxation event is more likely to take place when the density of free carriers is higher, which happens for high α. The Fill Factor (FF) and, consequently, the power efficiency (η) of the device are affected by Auger recombination (Table 2). As a result of this non-radiative phenomenon, the performance of the 3J solar cell is compromised, as shown in Fig 3 by the slow improvement in V_{oc} and the decay in the FF.

A maximum efficiency of 44.46% was found for a concentration of 100-suns (Table 2). The top subcell thickness was then optimized one more time and an improvement in the maximum current led to an efficiency of 51.75% (see simulated J-V curve in Fig 4).

The general behavior of the 3J device under concentrated sunlight depicted by the 1-dimensional device modeling is very realistic, resulting from the integration of recombination processes, which occur in real devices. Therefore, the modeling presented here is an important step towards the realization of all lattice-matched devices with optimized bandgap energies with ultra-high efficiencies.

V. CONCLUSION

Summarizing, we describe a new pathway for an all lattice-matched monolithic triple-junction device formed by (1.93 eV) InAlAs / (1.39 eV) InGaAsP / (0.94 eV) InGaAs compound semiconductors which allows for a very good

current-match, as shown by detailed balance calculations and device modeling. The performance of each subcell and the 3J device was analyzed by light J-V under AM 1.5D concentrated illumination. At 100-suns a maximum efficiency of > 51% was calculated. Auger recombination was found to play an important role for high-injection levels. The realistic device modeling presented here is an important step towards the development of the suggested 3J device, which is a promising option for CPV.

ACKNOWLEDGEMENT

The authors thank Spectrolab Inc. and J. N. Munday for fruitful discussions. The Department Of Energy (Solar Energy Technology Program under Grant No. DE-FG36-08GO18071) is acknowledged for funding. MSL acknowledges support under the Cooperative Research Agreement between the University of Maryland and the National Institute of Standards and Technology Center for Nanoscale Science and Technology, Award 70NANB10H193, through the University of Maryland.

REFERENCES

[1] R. R. King, D. C. Law, K. M. Edmondson, C. M. Fetzer, G. S. Kinsey, H. Yoon, R. A. Sherif, N. H. Karam, "40% Efficient Metamorphic GaInP/GaInAs/Ge Multijunction Solar Cells," *Applied Physics Letters*, vol. 90, pp. 183516, 2007.

[2] J. F. Geisz, S. Kurtz, M. W. Wanlass, J. S. Ward, A. Duda, D. J. Friedman, J. M. Olson, W. E. McMahon, T. E. Moriarty, J. T. Kiehl, "High-Efficiency GaInP/GaAs/InGaAs Triple-Junction Solar Cells Grown Inverted With a Metamorphic Bottom Junction," *Applied Physics Letters,* vol. 91, pp. 023502, 2007.

[3] P. Chiu, S. Wojtczuk, X. Zhang, C. Harris, D. Pulver, and M. Timmons, "42.3% Efficient InGaP/GaAs/InGaAs Concentrators using Bifacial Epigrowth," in 37th *IEEE PVSC*, 2011.

[4] M. Wiemer, V. Sabnis, and H. Yuen, ">41% efficient lattice matched solar cells, " in *Proceedings of SPIE*, vol. 8108, article 810804, 2011.

[5] R. J. Walters, M. González, J. G. Tischler, M. P. Lumb, J. R. Meyer, I. Vurgaftman, J. Abell, M. K. Yakes, N. Ekins-Daukes, J G. J. Adams, N. Chan, P. Stavrinou, and P. P. Jenkins, "Design of an Achievable, all Lattice-Matched Multijunction Solar Cell Using InGaAlAsSb," in *37th IEEE Photovoltaic Specialist Conference*, 2011.

[6] E. C. Warmann, M. S. Leite, and H. A. Atwater, "Photovoltaic Efficiencies in Lattice-Matched III-V Multijunction Solar Cells With Unconventional Lattice Parameters," in *37th IEEE Photovoltaic Specialist Conference*, 2011.

[7] M. S. Leite, E. C. Warmann, G. M. Kimball, S. P. Burgos, D. M. Callahan, and H. A. Atwater, "Wafer-Scale Strain Engineering of Ultrathin Semiconductor Crystalline Layers," *Advanced Materials*, vol. 23, pp, 3801-3807, 2011.

[8] R. L. Woo, W. D. Hong, S. Mesropian, M. S. Leite, H. A. Atwater, and Daniel C. Law, "First Demonstration of Monolithic InP-Based InAlAs/InGaAsP/InGaAs Triple Junction Solar Cells," in *37th IEEE Photovoltaic Specialists Conference*, 2011.

[9] R. Stangl, M. Kriegel, and M. Schmidt, "Afors-het, Version 2.2, a Numerical Computer Program for Simulation of Heterojunction Solar Cells and Measurements," in *4th IEEE World Conference on Photovoltaic Energy Conversion*, 2006, pp. 1350-1353.

[10] M. S. Leite, R. L. Woo, W. D. Hong, D. C. Law, D. C., and H. A. Atwater, "Wide-band-gap InAlAs solar cell for an alternative for multijunction approach," *Applied Physics Letters,* vol. 98, pp. 093502, 2011.

[11] M. S. Leite, R. L. Woo, W. D. Hong, D. C. Law, and H. A. Atwater, "InAIAs Epitaxial Growth for Wide Band Gap Solar Cells," in *37th IEEE Photovoltaic Specialist Conference*, 2011.